Cell, Vol. 87, 607–617, November 15, 1996, Copyright ©1996 by Cell Press

Absence Epilepsy in Tottering Mutant Mice Is Associated with Calcium Channel Defects

**Colin F. Fletcher,* Cathleen M. Lutz,†
T. Norene O'Sullivan,* John D. Shaughnessy, Jr.,*
Richard Hawkes,‡ Wayne N. Frankel,†
Neal G. Copeland,* and Nancy A. Jenkins***

*Mammalian Genetics Laboratory
ABL–Basic Research Program
NCI–Frederick Cancer Research
and Development Center
Frederick, Maryland 21702
†The Jackson Laboratory
Bar Harbor, Maine 04609
‡Department of Anatomy and Neuroscience
Research Group
Faculty of Medicine
University of Calgary
Calgary, Alberta T2N 4N1
Canada

Summary

Mutations at the mouse tottering (*tg*) locus cause a delayed-onset, recessive neurological disorder resulting in ataxia, motor seizures, and behavioral absence seizures resembling petit mal epilepsy in humans. A more severe allele, leaner (tg^{la}), also shows a slow, selective degeneration of cerebellar neurons. By positional cloning, we have identified an α_{1A} voltage-sensitive calcium channel gene that is mutated in *tg* and tg^{la} mice. The α_{1A} gene is widely expressed in the central nervous system with prominent, uniform expression in the cerebellum. α_{1A} expression does not mirror the localized pattern of cerebellar degeneration observed in tg^{la} mice, providing evidence for regional differences in biological function of α_{1A} channels. These studies define the first mutations in a mammalian central nervous system–specific voltage-sensitive calcium channel and identify the first gene involved in absence epilepsy.

Introduction

Approximately 1% of the human population suffers from some form of epilepsy. Epilepsies have one common defining feature, the recurrent synchronized discharges that interrupt the otherwise normal function of neuronal circuits, but vary in onset, severity, and etiology. Epilepsies are categorized as partial or generalized; generalized seizures are commonly known as grand mal (convulsive) or petit mal (absence). Because half of all epilepsies have an important genetic component, identification of mutations can be employed to define epileptogenic mechanisms. However, these efforts are complicated not only by clinical and genetic heterogeneity but likely by polygenic inheritance as well. Several human epilepsy genes have been mapped, but these do not represent the majority of idiopathic epilepsies (Anderson et al., 1991; Annegers, 1991; Hauser and Annegers, 1991; Ryan, 1995). In the mouse, a number of single gene mutations that cause epilepsy have been identified (Noebels, 1984a), and it is hoped that the identification and study of these genes will provide insights into human epilepsy.

One well-studied epileptic mouse mutation is the tottering (*tg*) locus on chromosome 8 (Green, 1989). The *tg* mutant strain is one of only a few known models for absence epilepsy. Absence epilepsy is recognized by behavioral arrest that accompanies generalized spike and wave discharges; also, the disease is uniquely responsive to ethosuximide. Tottering seizures are remarkably similar to human absence epilepsy: the mouse shows the characteristic behavioral arrest, assuming a fixed staring posture. Electroencephalographic recordings are normal except during the frequent, spontaneous seizures when generalized, bilateral spike and wave discharges are observed. In addition, *tg* mice are responsive to antiabsence drugs (Hellar et al., 1983). Histological examination of *tg* mice has revealed one cytological alteration: noradrenergic fibers of the locus ceruleus hyperinnervate the central nervous system (CNS) (Levitt and Noebels, 1981).

The tottering phenotype also includes motor seizures and ataxia. Spontaneous motor seizures occur infrequently in *tg* mice and are characterized by a stereotyped, progressive involvement of all limbs that occurs over 20–30 min (Green and Sidman, 1962). An initial clonic phase involving only the hindlimbs often spreads to tonic/clonic involvement of the forelimbs and trunk before ending abruptly. No particular abnormality of electroencephalographic recordings has been associated with these seizures (Noebels and Sidman, 1979).

The ataxic behavior of *tg* mice includes a splayed stance and hopping gait, with a tendency to hold the tail arched over the back. This behavior is manifested around the third postnatal week; histological examination has not detected gross cytoarchitectural defects in the cerebellum or brain stem. In older mice, some shrinkage of Purkinje cells is detected by electron microscopy (Meier and MacPike, 1971). Tyrosine hydroxylase (TH), a key enzyme in the noradrenergic biosynthesis pathway, has been shown to be persistently expressed in cerebellar Purkinje cells in the *tg* mouse (Hess and Wilson, 1991).

Two additional *tg* mutations have been identified that present different but overlapping features. Similar to *tg*, leaner (tg^{la}) mice suffer from absence seizures (Noebels, 1984b) and the cellular phenotype of aberrant TH gene expression (Hess and Wilson, 1991), but they do not have motor seizures. Leaner mice are severely ataxic and often do not survive past weaning. These mice show a degeneration of differentiated granule, Golgi, and Purkinje cells within the cerebellum that progresses slowly over a period of months (Herrup and Wilczynski, 1982). The degeneration selectively affects a subset of Purkinje cells in the cerebellum in a longitudinally striped pattern that is similar to the pattern of zebrin expression (Hawkes and Gravel, 1991; Heckroth and Abbott, 1994).

Mice carrying the rolling Nagoya (tg^{rol}) allele present an intermediate phenotype; the ataxia is somewhat more severe than with *tg*, and motor seizures do not occur.

Locus ceruleus hyperinnervation (Adachi et al., 1975) and cerebellar degeneration have been reported (Nishimura, 1975), however, *tg*^{rol} animals have a normal life span.

In this study, we have employed a positional cloning strategy to identify a voltage-sensitive calcium channel of the α_{1A} subtype that is mutated in *tg* mice. Voltage-gated calcium channels are widely expressed, multisubunit complexes, which, in addition to electrogenic roles, have unique signal transduction functions that regulate a variety of neuronal functions (Hille, 1992). A combination of electrophysiological and pharmacological criteria have defined five main types of high threshold calcium channels (L, N, R, P, and Q) whose pore-forming subunits are encoded by a small gene family (A, B, C, D, E, and S) (for review, see Catterall, 1995; Dunlap et al., 1995). While there is still some debate, it appears likely that the α_{1A} calcium channel is a major component of the P- and Q-type calcium channels (Sather et al., 1993; Stea et al., 1994). P- and Q-type channels were first described in cerebellar neurons and have been implicated in neurotransmitter release (Llinas et al., 1989a; Zhang et al., 1993). The identification of the α_{1A} channel as the product of the *tg* locus provides a physiological basis for understanding the phenotype of *tg* mice and implicates the high threshold class of calcium channels in epilepsy.

Results

Fine Structure Mapping of *tg*

The *tg* locus was fine mapped on mouse chromosome 8 using two intersubspecific crosses. In the first cross, (B6.D2-*tg/tg* X CAST/Ei)F_1 mice were backcrossed to B6.D2-*tg/tg* mice to produce 600 backcross progeny that were scored for their *tg* phenotype. In the second cross, B6.AKR-*tg*^{la} +/+ *Os* mice were mated to CAST/Ei mice, and heterozygous *tg*^{la} F_1 animals were intercrossed to produce 1100 F_2 progeny. *Os* is a tightly linked semidominant skeletal mutation (Green, 1989) carried in repulsion with *tg*^{la}. Heterozygous *Os*/+ F_1 mice were identified by observation of the oligosyndactylism phenotype, thus allowing the *tg*^{la} genotype of unaffected heterozygous F_1 animals to be inferred. Intercross progeny were scored for their *tg*^{la} phenotype, and unaffected animals harboring key recombinant chromosomes were genotyped by progeny testing through mating to heterozygous *tg*^{la} mice. High resolution genetic linkage maps encompassing both microsatellite and gene-based restriction fragment length polymorphism (RFLP) markers were then generated from both crosses (Figure 1).

Congenic analysis was also performed on the *tg* and *tg*^{la} strains. Both mutations have been moved from their strain of origin (DBA/2J for *tg*; AKR/J for *tg*^{la}) to C57BL/6J by repeated backcrossing and selection for mutant animals (49 backcrosses for *tg*; 40 backcrosses for *tg*^{la}). The congenic segment retained in the backcross progeny can be defined by RFLP and microsatellite analysis and can provide useful information for positional cloning (Figure 1). Among five markers (lymphoblastic leukemia 1 [*Lyl1*], nuclear factor I/x transcription factor [*Nfix*], *Junb*, glutaryl CoA-dehydrogenase [*Gcdh*], and *D8Mit283*) found to be nonrecombinant with *tg* in the backcross (Figure 1), only one (*Lyl1*) was DBA-like, placing

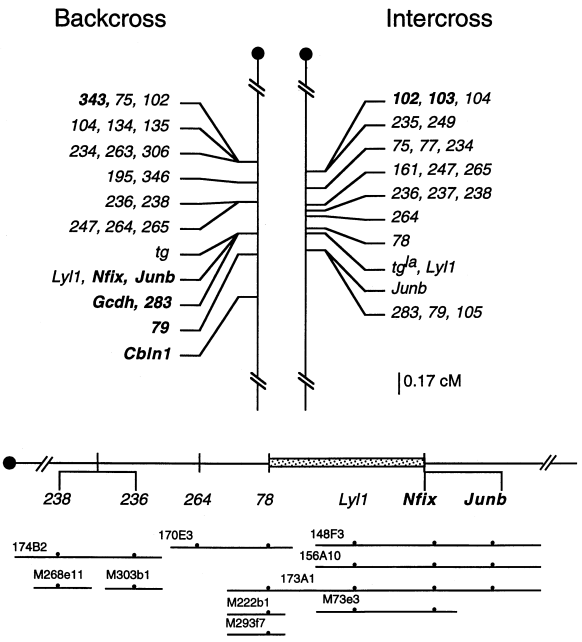

Figure 1. Genetic and Physical Maps Define the *tg* Critical Region

The fine structure linkage map of *tg* was determined by backcross and intercross analysis. Partial chromosome linkage maps show the location of the *tg* and *tg*^{la} alleles in relation to linked markers. MIT markers are indicated by number; the "D8Mit" prefix has been omitted for legibility. Markers in bold were typed as B6 in the *tg* and *tg*^{la} congenic strains. Centromere is indicated by filled dot, and genetic distance is to scale. A partial chromosome map showing the disposition of genetic markers and YAC clones (horizontal lines) is indicated. Marker content is indicated by bullets on the YACs. The stippled box indicates the region that must contain the *tg* locus.

the other four markers immediately distal to *tg*. Two of these markers (*Junb* and *D8Mit283*) were typed in the intercross and confirmed to lie distal of *tg* (Figure 1). The closest proximal marker to *tg*, *D8Mit78*, was defined in the intercross, where it was predicted to lie 0.04 ± 0.05 cM proximal to *tg*^{la} (Figure 1). Only the *Lyl1* locus remained nonrecombinant with *tg* in the backcross/intercross and congenic analyses.

Physical Cloning of the *tg* Interval

Physical cloning of the *tg* interval was accomplished by screening several yeast artificial chromosome (YAC) libraries using the microsatellite markers and cDNA probes flanking the *tg* locus (Figure 1). One *Lyl1*-positive YAC clone, M73e3, was positive for *Nfix* but not *Junb*, placing *Nfix* proximal to *Junb*. One YAC clone, 173A1, spanned the *tg* interval, as it was positive for *D8Mit78* and *Nfix*, although we have determined that it is internally deleted. In the course of gene-trapping and physical-mapping experiments, a proximal endclone of M73e3 was isolated by inverse polymerase chain reaction (PCR) and sequenced. A database search revealed the presence of 38 nucleotides that matched positions 6157 to 6195 of the rat α_{1A} voltage-sensitive calcium channel gene. Flanking splice donor and acceptor consensus sequences suggested that this was a bona fide exon of the homologous mouse gene.

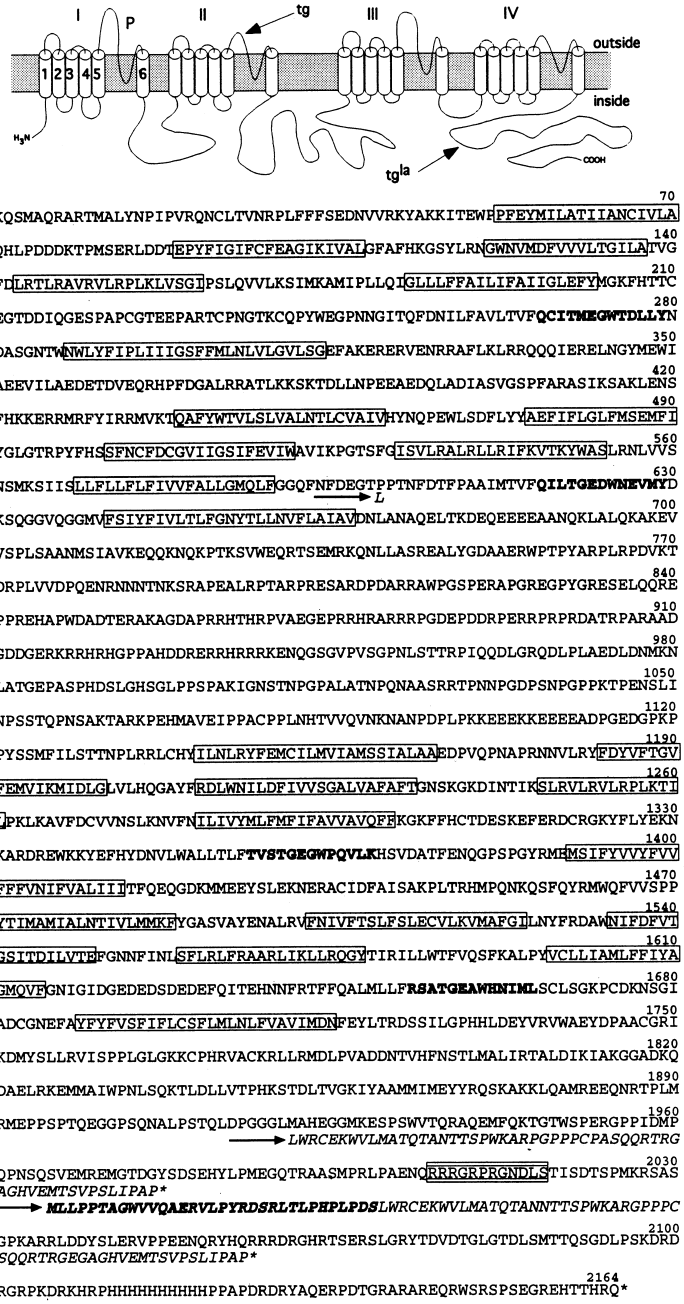

Figure 2. Topology and Sequence of the Mouse α_{1A} Gene

Depiction of the proposed topology of the α_{1A} gene. The shaded area indicates cellular membrane, with cylinders indicating transmembrane domains. Repeats (I–IV) of 6 transmembrane segments (1–6) and a P domain are organized in tetrad symmetry to form a single ion channel. Positions of *tg* and *tg*^{la} mutations are indicated by arrows. Predicted amino acid sequence of the α_{1A} cDNA open reading frame. Presumed transmembrane domains, identified by similarity to rat and rabbit genes, are indicated by boxes. Repeats of transmembrane clusters are indicated to the left (I–IV, vertical lines in the left margin). Conserved sequence that is part of the P domain is indicated in bold. The position of amino acid change (1802, P to L) in *tg* is indicated by an arrow. Positions of altered amino acid sequences in *tg*^{la} are indicated by arrows (1922 and 1968), with novel sequences in italic. The sequence in bold italic represents intron translation; plain italic is out-of-frame translation of exon sequence. The double box indicates exon first discovered in the M73e3 YAC endclone. Termination codons are represented by asterisks.

Characterization of the Mouse α_{1A} Gene

Evaluation of the calcium channel gene as a candidate for the *tg* locus was initiated by cloning the mouse homolog by reverse transcription–PCR (RT–PCR) using primers based on the rat sequence. Sequence analysis of derived clones yielded a consensus sequence containing an open reading frame of 6492 nucleotides encoding a predicted protein of 2164 amino acids (Figure 2). This sequence is most similar to the rat and rabbit genes of the α_{1A} subtype. Specifically, the tg clone is 96% and 90% identical to the rat and rabbit α_{1A} genes, respectively, while no more than 80% identical to other α_1 genes. The predicted peptide contains conserved regions that are thought to be transmembrane segments, grouped in four domains of six transmembrane regions each (Figure 2) (Tsien et al., 1991). The pore-lining (P) domains also show conserved sequence motifs, including the four glutamate residues thought to line the pore in a staircase fashion and confer Ca^{2+} selectivity (Tang et al., 1993; Yang et al., 1993). Northern blot analysis revealed major transcripts of 8.2 and 8.6 kb and suggested that α_{1A} expression is brain specific (Figure 3). Backcross, intercross, and congenic analysis localized the calcium channel gene to the *tg* interval (data not shown).

α_{1A} Defects in *tg* Mutant Mice

Northern blot analysis of cerebellar RNA failed to reveal any differences in α_{1A} expression in *tg* or *tg*^{la} mutant mice

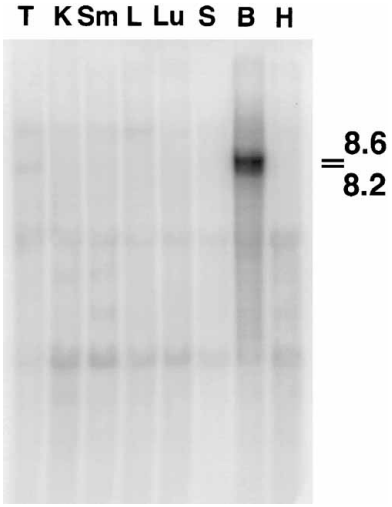

Figure 3. α_{1A} Expression in Adult Mouse Tissues

Mouse polyA+ Northern blot was probed with a fragment of the α_{1A} gene corresponding to nucleotides 5426–6031. Lanes are (T) testes, (K) kidney, (Sm) skeletal muscle, (L) liver, (Lu) lung, (S) spleen, (B) brain, and (H) heart. Specific hybridization was only observed with brain RNA. Transcript sizes are indicated in kilobases at the right. On most gels, a doublet was observed; occasionally, a faint band of approximately 12 kb is also detected.

(Figure 4A). A series of RT-PCR fragments spanning the transcript were generated; this survey detected an alteration in the 3′ end of the *tg*^{la} transcript (Figure 4B). Primers located at positions 5653 and 5923 generated a wild-type 270 bp RT-PCR fragment, while aberrant bands of larger and smaller size and little or no wild-type size fragment were seen in the *tg*^{la} sample. Both gel-purified fragments were sequenced: the larger fragment contained an insertion of 98 nucleotides at position 5901/2, while the smaller fragment had a deletion of 139 nucleotides (nt 5763–5901). Genomic sequence analysis identified intron/exon junctions at positions 5762/3 and 5901/2. Thus, the larger fragment results from failure to splice out an intron, while the smaller fragment results from skipping of one exon (Figure 4C). Both transcripts are predicted to produce abnormal proteins. The exon skip results in an out-of-frame splice, while intron inclusion results in translation of the intron sequence and an out-of-frame read through of subsequent exons. Genomic sequencing of AKR/J, C57BL/6J, and B6.AKR-*tg*^{la}/*tg*^{la} DNA revealed a single G-to-A change in *tg*^{la} DNA, located in the splice donor consensus sequence at the 5′ end of the unspliced intron (Figure 4C). Multiple aberrant transcripts are commonly associated with these types of mutations (Krawczak et al., 1992). Use of an intron B-specific primer in RT-PCR yielded product only from *tg*^{la} RNA (data not shown).

No alterations in transcript structure were found in *tg* mice, so nucleotide sequence analysis was performed. The *tg* transcript contained a C-to-T change at position 1802, relative to the control DBA/2J sequence (Figure 4D). This alteration leads to a nonconservative proline-to-leucine amino acid substitution in a position very close to the conserved P domain (Figure 2). The position and nature of this mutation suggest that pore function is altered in the *tg* strain.

α_{1A} Expression

The relationship between α_{1A} expression in the central nervous system and the phenotype of *tg* mutant strains was analyzed by in situ hybridization. Sense and antisense riboprobes were generated from the α_{1A}-specific 3′ terminus (nt 5425–6051). Hybridization to sagittal brain sections revealed widely distributed expression (Figure 5A; control strand Figure 5B). Moderate to high levels of expression were observed in the olfactory bulb, the cerebral cortex, the hippocampus, the inferior colliculus, and the cerebellum. Dense labeling was apparent throughout all layers of the cerebral cortex, and there was strong expression in the pyramidal and granule neurons, as well as interneurons, of the hippocampus (Figure 5C). In the cerebellum, prominent expression was detected in Purkinje and granule cells. Labeling was observed in the deep cerebellar nuclei but not in the molecular layer or white matter (Figure 5D). Expression was also observed in two areas from which cerebellar afferents arise, the pontine and inferior olivary nuclei (Figure 5A). Relative to the localized cell death and TH expression seen in the *tg*^{la} cerebellum (see below), α_{1A} expression was uniform across the cerebellum (Figure 5E).

Localized Cell Death and TH Expression in the Leaner Cerebellum

In contrast to the uniform α_{1A} expression observed in the cerebellum, Purkinje cell degeneration seen in the *tg*^{la} cerebellum is nonuniform and occurs in parasagittal stripes separated by areas of normal nondegenerating cells (Heckroth and Abbott, 1994) (Figure 6J). We observe that the pattern of surviving Purkinje cells is essentially coextensive with the pattern seen when the mouse cerebellum is stained with antibodies to markers such as zebrin (Hawkes and Gravel, 1991) (Figures 6B, 6E, 6H, and 6K). Zebrin is the prototype of a small collection of markers that are expressed in this striped pattern, which is thought to reflect an inherent higher order functional organization of the cerebellum that is not visible by simple light microscopic analysis alone (Hawkes and Gravel, 1991). Additional evidence for regional differences in α_{1A} function comes from TH expression studies. In *tg* and *tg*^{la} mice, the normally transient expression of TH is not suppressed, resulting in expression in the adult (Hess and Wilson, 1991; Austin et al., 1992). While the ectopic TH expression seen in *tg* and *tg*^{la} mice has been described as "patchy," we have found that it is coextensive with zebrin staining (compare Figures 6F and 6I with Figures 6E and 6H). It is interesting to note that the TH expression patterns are similar in the *tg* and *tg*^{la} cerebellum (Figure 6F versus Figure 6I) even though the *tg* cerebellum does not undergo the extensive Purkinje cell degeneration seen in the *tg*^{la} cerebellum (Figure 6D versus Figures 6G and 6J). Thus, the two cellular phenotypes are not unrelated, but in fact, both observe a common boundary that distinguishes two populations of Purkinje cells.

Chronic derangement of calcium homeostasis has been shown to induce a slow, progressive apoptotic cell death (Limbrick et al., 1995). To determine if this could explain the cerebellar degeneration seen in *tg*^{la} mice,

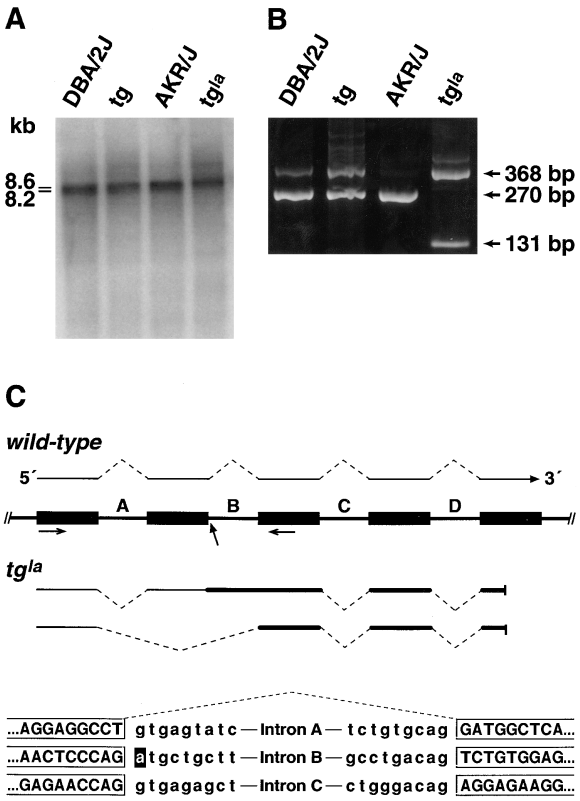

Figure 4. Expression and Structure of the α_{1A} Gene in *tg* and *tg*^{la} Mutant Mice

(A) α_{1A} expression in wild-type, *tg*, and *tg*^{la} mice. Poly A+ RNA (2 μg), prepared from cerebella of DBA/2J, B6.D2-*tg*/*tg*, AKR/J, and B6.AKR-*tg*^{la}/*tg*^{la} mice, was electrophoresed in a formaldehyde-acrylamide gel, transferred to nylon membrane, and probed with an α_{1A} tail region probe corresponding to nucleotides 5426–6031. Hybridization signals were quantitated using a Storm 860 Phospholmager. A glyceraldehyde 3-phosphate dehydrogenase probe was hybridized to the blot to normalize RNA loading. No differences in expression level were observed. Occasionally, a faint band of approximately 12 kb is observed.

(B) Analysis of α_{1A} expression in wild-type, *tg*, and *tg*^{la} mice by RT-PCR. First strand cDNA was synthesized from total RNA prepared from cerebella of DBA/2J, B6.D2-*tg*/*tg*, AKR/J, and B6.AKR-*tg*^{la}/*tg*^{la} mice and amplified by PCR with primers located at nucleotide positions 5653 and 5923. *tg*^{la} RNA showed an alteration in fragment size, such that only fragments that were larger and smaller than wild type were synthesized. Fragment sizes are indicated on the right. A variable, faint, larger band was occasionally seen in all samples.

(C) Intron/exon and transcript structure in normal and *tg*^{la} strains. The central line with open boxes indicates α_{1A} genomic structure; boxes are exons, and introns are thin lettered lines. Transcripts are indicated above and below as thin lines; these are wild type and *tg*^{la}, respectively. Splicing events are indicated by dashed lines. Transcript regions encoding novel peptide sequences are indicated by thick lines, with translation stops indicated as thick vertical lines. Horizontal arrows represent PCR primers, and the vertical arrow indicates the position of splice donor mutation in *tg*^{la} mice. The sequence of intron/exon junctions is shown below, with exon sequences as all capital letters and intron sequences in lowercase. *tg*^{la}-specific adenosine in intron B splice donor is in reverse bold.

(D) Sequence alteration in a *tg* strain. Nucleotide and predicted amino acid sequence of wild type (above) and *tg* (below) are shown. *tg* contains a cytosine to thymidine change at position 1802, which results in a proline to leucine change in the predicted amino acid sequence.

we used the TUNEL assay (Gavrieli et al., 1992) to analyze these mice for evidence of apoptotic cell death. This assay detects, in situ, double-strand DNA breaks, which are associated with apoptotic cell death. Stained sections of tissue from 38 day postnatal wild-type control and *tg*^{la} animals are shown in Figure 7. No stained cells were seen in the normal controls (Figure 7A), but strongly stained granule neurons were distributed throughout the internal granule cell layer of *tg*^{la} mice (Figure 7B). Rare stained Purkinje cells were also observed. Staining at 38 days postnatally was more extensive than postnatal days 26 or 70, consistent with quantitative observations on the rate of granule cell loss in the *tg*^{la} cerebellum (Herrup and Wilczynski, 1982). The high sensitivity of this assay was exploited to search for other affected regions in the *tg*^{la} brain. Horizontal sections, which spanned most of the brain (dorsal surface to midspine level) from the three ages, were examined, and in no case was any significant staining discovered.

Discussion

tg Encodes a Voltage-Sensitive Calcium Channel

We have presented evidence that the *tg* locus encodes a voltage-sensitive calcium channel. First, the α_{1A} gene is located in a genetic interval of <0.07 cM, defined by congenic, backcross, and intercross analysis, that must contain the *tg* locus. In addition, the α_{1A} gene is expressed in the brain, the tissue affected in *tg* mice. Second, we have discovered genetic alterations, specific to the *tg* and *tg*^{la} strains, that alter the coding sequence of the calcium channel gene, relative to the known chromosomes of origin. Specifically, the *tg*^{la} allele contains a mutation of a splice donor consensus that results in truncation of the normal open reading frame at amino acid positions 1922 or 1968 and expression of novel carboxy-terminal sequences. The *tg* allele contains a single nucleotide change that results in a nonconservative amino acid change near the second P domain.

tg Is the Mouse α_{1A} Subtype Gene and Encodes a P/Q-Type Channel

High threshold voltage-sensitive calcium channels are multisubunit complexes that comprise an α_1 protein, which forms the channel per se, and additional regulatory-accessory proteins, including the β, α_2-δ, and γ proteins. Isolation of α_{1S} cDNA clones led to identification of five additional genes: α_{1A}, α_{1B}, α_{1C}, α_{1D}, and α_{1E}. The *tg* gene is most similar to α_{1A} genes of rat and rabbit (Mori et al., 1991; Starr et al., 1991). Consistent with observations in other species (Mori et al., 1991; Stea

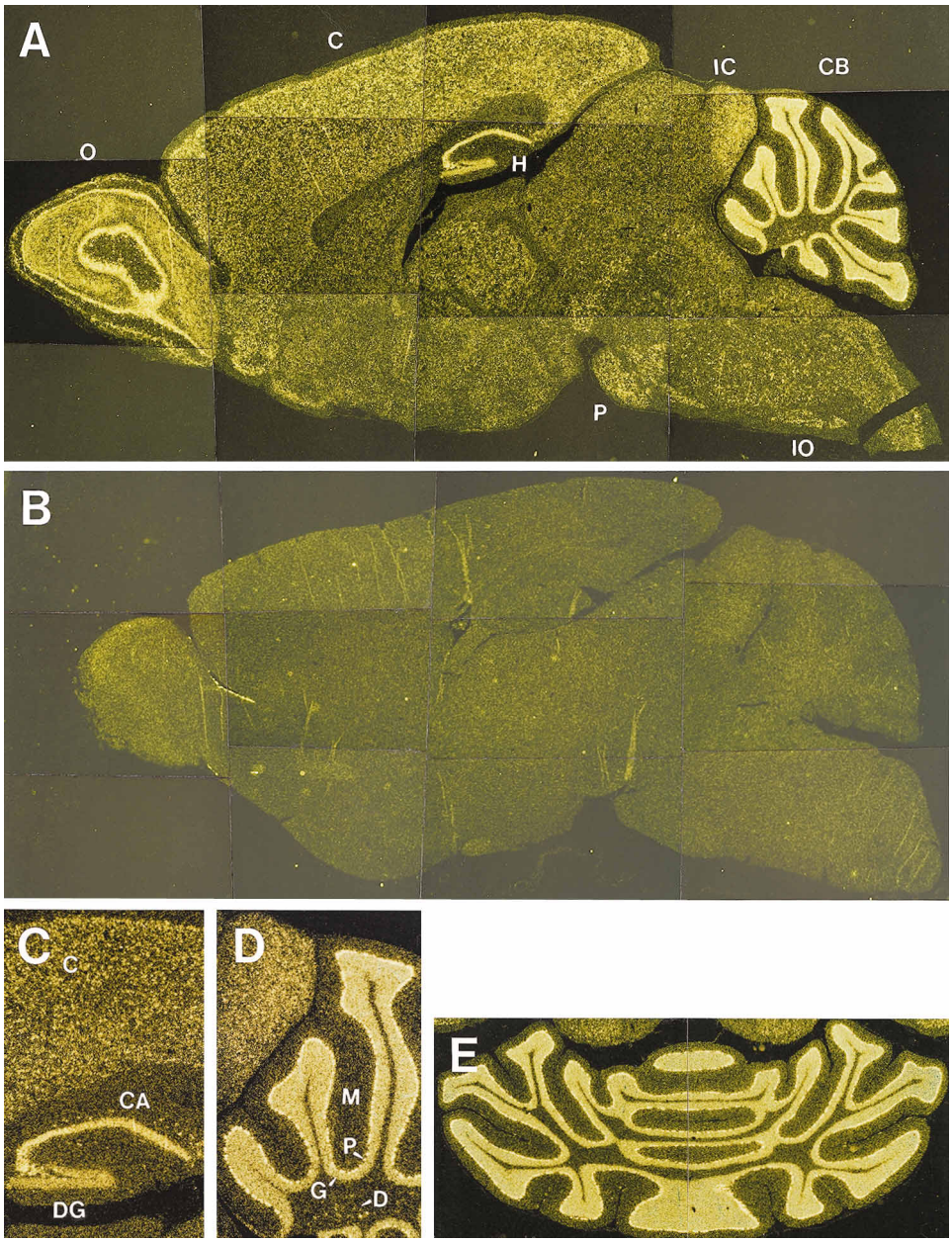

Figure 5. In Situ Analysis of α_{1A} Expression in the Mouse CNS

(A and B) Analysis of sagittal sections of wild-type mouse sections with (A) antisense and (B) sense (control) probes corresponding to nucleotides 5426–6031 of the mouse α_{1A} gene. Moderate to high levels of expression are seen in the olfactory bulb (O), cerebral cortex (C), hippocampus (H), inferior colliculus (IC), pontine nucleus (P), cerebellum (CB), and inferior olivary nucleus (IO). No specific signal is detected with the control probe.

(C) Higher power images of the forebrain, including the cerebral cortex and hippocampus. Signals are seen throughout the cerebral cortex (C), in the cornu ammonis pyramidal neurons (CA), and the granule cells of the dentate gyrus (DG), as well as scattered interneurons (outlying cell bodies).

(D) Higher power images of the cerebellum. Expression is absent in the molecular layer (M) but is strong in the Purkinje cell bodies (P), the granule cell layer (G), and the cell bodies in the deep cerebellar nuclei (D).

(E) Higher power images of horizontal section show uniform expression in all Purkinje and granule neurons throughout the cerebellum.

et al., 1994; Volsen et al., 1995), the *tg* gene is widely expressed in the mouse CNS: in situ analysis detects expression in the cerebral cortex, hippocampus, olfactory bulb, tectum, and hindbrain, with strong expression in cerebellar granule and Purkinje cells.

A variety of calcium channels, designated L, N, P, Q, T, and R, are expressed in neuronal, endocrine, vascular, and cardiac tissue as well as skeletal muscle. P-type channels were originally identified as the dominant calcium current in Purkinje cells (Llinas et al., 1989a), whereas Q-type channels were first identified in cerebellar granule cells (Zhang et al., 1993). P- and Q-type

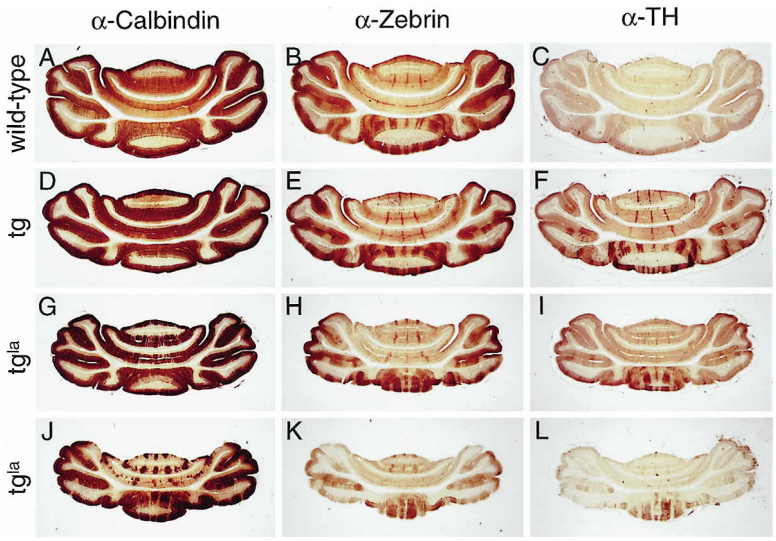

Figure 6. Localized Cell Death and TH Expression in *tg* and *tg*^{la} Cerebella

Distribution of Purkinje cells (A, D, G, and J) and expression of zebrin (B, E, H, and K) and TH (C, F, I, and L) in wild-type (A–C), *tg* (D–F), and *tg*^{la} (G–I, postnatal day 42; J–L, postnatal day 140) cerebella. Selective loss of Purkinje cells in aged *tg*^{la} in alternating bands can be seen in (J), compared to no cell loss in wild-type (A) and *tg* (D) and little cell death at postnatal day 40 in *tg*^{la} (G). Striped expression of zebrin can be seen in all samples (B, E, H, and K). Expression of TH is seen in *tg* (F) and *tg*^{la} (I and L) but not in wild-type (C) in a pattern similar to zebrin. Purkinje cells were visualized by immunostaining with antisera to Calbindin, a 28 kDa calcium-binding protein, which, in the cerebellum, is expressed only in these cells (Christakos et al., 1987). The distribution of zebrin-positive and TH-positive cells was similarly determined using anti-zebrin and anti-TH antisera in sequential sections.

channels are distinguished by their pharmacological profiles and electrophysiological properties (Llinas et al., 1989b). Proteins encoded by the α_{1A} gene are thought to give rise to P- and/or Q-type calcium currents, in part because of the α_{1A} expression pattern (Wheeler et al., 1995). Interestingly, cloned α_{1A} transcripts expressed in heterologous cells (e.g., Xenopus ooctyes) give rise to channels with properties intermediate to the P and Q

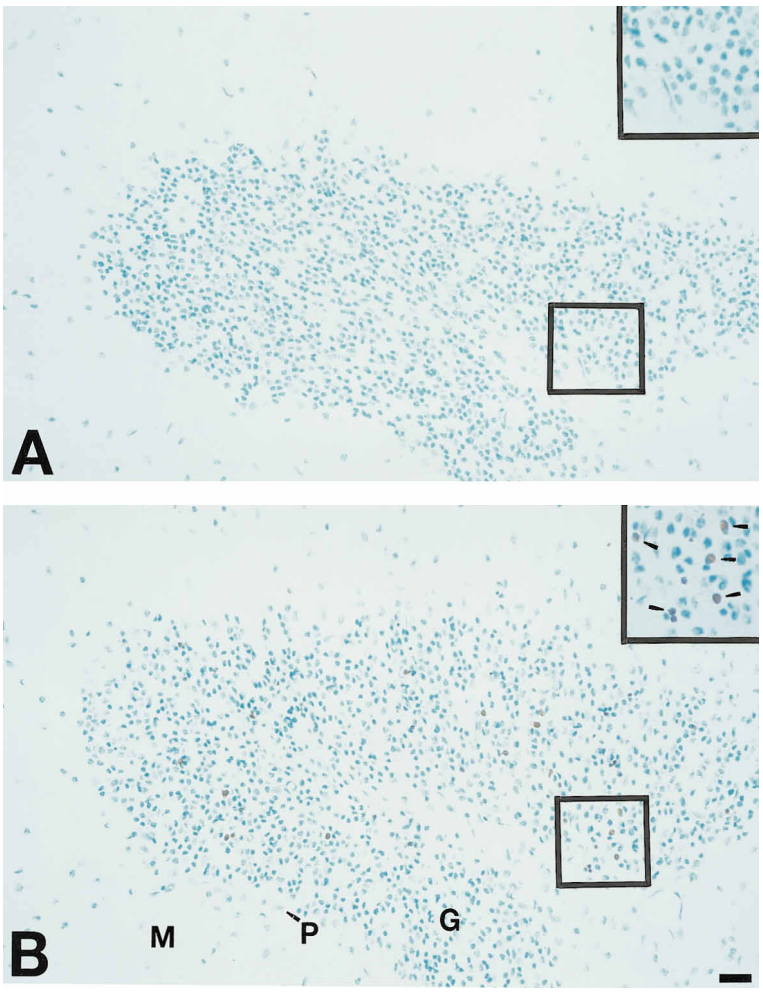

Figure 7. Apoptotic Cell Death in the *tg*^{la} Cerebellum

Wild-type (A) and *tg*^{la} (B) sections immunostained with anti-digoxigenin antisera after terminal transferase tailing with digoxigenin-UTP in situ. Immunostaining is purplish-brown; the sections are counterstained with toluidine blue. The *tg*^{la} cerebellum shows significant staining of granule cells (G); see also the higher magnification inset. Purkinje cells (P) are occasionally stained. No staining is observed in the molecular layer (M) or in sections from wild-type mice. Scale bar, 25 μm.

channels detected in the mammalian CNS (Sather et al., 1993; Stea et al., 1994). Thus, the exact relationship between this gene and functionally identified channel activities is not entirely clear.

In Vivo Function of the α_{1A} Channel

In addition to an electrogenic role, voltage-sensitive calcium channels serve as the sole coupling of electrical activity to cellular biochemical function. This transducing function results from the biological activity of the calcium ion, which, upon entry into the cell, acts as a second messenger to modulate cellular functions such as secretion, contraction, migration, excitability, and gene expression (Hille, 1992). The most well-characterized function is coupling depolarization and neurotransmitter secretion at the presynaptic nerve terminal. Studies using brain slice preparations in vitro indicate a role for P and Q channels in excitatory transmission (Takahashi and Momiyama, 1993; Wheeler et al., 1995). However, these channels have also been detected in dendrites and cell bodies and thus act postsynaptically as well (Usowicz et al., 1992).

Compared to the wealth of in vitro data, relatively little is known about channel function in intact animals. Only one mutation affecting a voltage-sensitive calcium channel has been described. The muscle-specific α_{1S} subunit is truncated in the muscular dysgenesis mouse (Chaudhari, 1992), resulting in failure of myoblast differentiation. Point mutations in the human homolog have been shown to cause hypokalemic periodic paralysis (Ptacek et al., 1994). Additional information about in vivo function has been derived from study of patients with Lambert-Eaton myasthenia syndrome, in which behavioral symptoms are correlated with the presence of anticalcium channel autoimmune antibodies in the sera, indicating a role in excitatory transmission in the peripheral nervous system (Lennon et al., 1995).

Elucidating the contribution of these channels to neuronal function in the intact animal is of great interest, and identification of mutations in the α_{1A} gene in the *tg* mouse provides a unique opportunity to investigate calcium channel function in the CNS in vivo. The constellation of defects that constitute the *tg* phenotype are largely consistent with the functions of calcium channels predicted from in vitro experiments. There is ample precedent for calcium involvement in neuronal cell death (Orrenius and Nicotera, 1994; Choi, 1995). Our observation of strong TUNEL staining in granule cells, taken together with previous morphological descriptions, is consistent with an apoptotic response and is suggestive of decreased intracellular calcium levels (Koh and Cotman, 1992; Galli et al., 1995). A role for calcium channel function in synapse maturation is consistent with observations about calcium effects on growth cone behavior (Kater and Mills, 1991; Spitzer et al., 1994; Zheng et al., 1994). Interestingly, this defect is not a secondary effect of hyperexcitability but is *tg* gene specific, as it is not seen in other epileptic mice (Qiao and Noebels, 1991). The persistent expression of TH is consistent with the known effect of calcium in regulating immediate early gene expression (Ghosh et al., 1994) and the responsiveness of the TH promoter to c-*fos*, calcium, and neuronal activity (Gizang-Ginsberg and Ziff, 1990; Kilbourne et al., 1992).

What is unexpected, however, is the remarkably restricted expression of the *tg* mutation. This is most clearly illustrated by the cerebellar phenotypes: misregulated TH gene expression and cellular degeneration only affect particular subsets of Purkinje cells. Similarly, the aberrant synaptogenesis of locus ceruleus neurons in *tg* mice is not a systemic effect on CNS neurons. The widespread expression of the channel demonstrates that this specificity is not simply due to differential expression of the α_{1A} gene. These observations are not predicted by previous electrophysiological or molecular characterization of calcium channels and imply that there are specific functions of calcium channels in particular neurons. The observed specificity could be accomplished by a number of mechanisms. Channel activity could be directly modulated by differential expression of functional isoforms of the channel in particular neurons. Although many differences in molecular transcripts of calcium channels have been described (Perez-Reyes and Schneider, 1995), evidence that these correspond to functional isoforms is only currently emerging (Rettig et al., 1996). Modulation may also be achieved by differential expression of the other channel subunits, which are known to affect channel properties. In a similar vein, overlapping expression of other pore-forming genes may contribute to specificity. Finally, factors extrinsic to the channel complexes per se, such as upstream modulators, downstream targets, or calcium-buffering proteins, may underlie the specific biological effects of the calcium channel in different cells. Identification of the mechanism responsible for the differential sensitivity of these cells to neuronal insult may provide insight into other forms of selective neuronal degeneration.

α_{1A} Mutations Underlie Absence Epilepsy

Likewise, the observation that a high threshold calcium channel mutation results in epilepsy is unexpected. Epileptic seizures result from an altered network property of neuronal circuits that results in intermittent, synchronized bursting of neurons separated by periods of normal function. In absence epilepsy, experimental studies and clinical observations indicate a central role of a thalamocortical circuit in the genesis of bilateral cortical spike and wave discharges (de Curtis and Avanzini, 1994; Snead, 1995). This circuit comprises only three neuronal populations: cortical pyramidal neurons, thalamic relay neurons, and neurons of the nucleus reticularis thalami. The interplay between γ-aminobutyric $acid_B$–mediated inhibition and the low threshold T-type calcium channel plays a critical role in generating the oscillating hyperpolarization/depolarization activity seen in the thalamus. The multigenic rat model of absence epilepsy (GAERS; Marescaux et al., 1992) has an increase in T-type calcium conductance (Tsakiridou et al., 1995). This is thought to promote intrathalamic burst activity and may even be the primary defect underlying seizure generation. These observations raise questions about the relationship between the yet uncloned T-type channel and the α_{1A} gene identified here. It is possible that the *tg* lesions have an indirect effect on T-channel function. Alternatively, it is conceivable that the α_{1A} gene additionally encodes a low threshhold isoform. In either case, the data presented here identify for the first time a gene

involved in absence epilepsy and define a trigger for seizure generation.

Experimental Procedures

Mice

The B6.D2-*tg* +/+ *Os*, B6.AKR-*tg*^{la} +/+ *Os*, AKR/J, DBA/2J, and CAST/Ei mice were maintained and propagated at ABL–Basic Research Program, Frederick, Maryland, and at the Jackson Laboratory, Bar Harbor, Maine.

Southern Analysis

Southern blot analysis was performed essentially as described (Jenkins et al., 1982). All probes were labeled with α^{32}P-dCTP using a random prime labeling kit (Amersham) or nick translation kit (Boehringer Mannheim); washing was done in 0.5–1.0 X SSC, 0.1% SDS at 65°C.

Intersubspecific Backcross and Intercross Mapping

Intersubspecific backcross progeny were generated as described (see Results). Strain DNAs were digested separately with several enzymes and analyzed by Southern blot hybridization for RFLPs. The inheritance pattern of each RFLP was then determined by following the presence or absence of each strain-specific RFLP in backcross and intercross mice. The *Lyl1* probe (Mellentin et al., 1989) was a 3.5 kb BamHI/EcoRI fragment of mouse cDNA. The *Gcdh* probe (Koeller et al., 1995) was a 1.75 kb EcoRI/XbaI fragment of mouse cDNA. The *Junb* proto-oncogene (*Junb*) probe (Ryder et al., 1988) was a 1.8 kb EcoRI fragment of mouse cDNA. The *Nfix* probe (Qian et al., 1995) was a 0.65 kb EcoRI fragment of mouse cDNA. The cerebellin (*Cbln1*) probe (Urade et al., 1991) was a 0.6 kb BamHI/HindIII fragment of mouse cDNA. The α_{1A} calcium channel (*Ccha1a*) probe, a PCR-generated fragment, corresponds to nucleotides 5426–6031. Recombination distances and gene order were calculated using the computer program Map Manager (written by Dr. K. Manley).

YAC Screen and Inverse PCR Cloning

YAC library DNA pools (MIT/Whitehead library) were obtained from Research Genetics (Huntsville, AL) and the Baylor University Genome Center (St. Mary's Library, indicated by "M" prefix) and screened with MIT primer pairs according to manufacturer's instructions. Gene-specific primers included: TGTCAGTTCACAAGCCACA GCT and AGTACAGCCAGGTGCTTATGAG (Junb) and GACCAAACG GCTGTGCTGACCT and AGGGACGTCTGCTCCAACTTGA (Lyl1). An M73e3 YAC endclone was obtained by inverse PCR. Total yeast DNA was digested with BstUI and ligated overnight at a concentration of 10 μg/ml. PCR was performed using the Expand High Fidelity kit (Boehringer Mannheim) according to manufacturer's instructions. Right-arm primers were CAUCAUCAUCAUATCTCCCGGGGCGATC GAACG and CAUCAUCAUCAUATCACCGATGGGGAAGATCGGG. The PCR fragment was gel purified and cloned into pAMP1 using the UDG cloning kit (GIBCO/BRL) according to the manufacturer's instructions.

Sequence Analysis

Sequencing was performed using PRISM ReadyReaction DyeDeoxy Terminator Cycle-sequencing Kit with Amplitaq-FS (Perkin Elmer), and data were acquired on an ABI Model 377 DNA sequencer (Applied Biosystems). Sequence was also obtained manually using Amplicycle Sequencing Kit (Perkin Elmer) with α^{32}P incorporation according to the manufacturer's instructions. Sequence reactions were electrophoresed through a 6% acrylamide denaturing gel (Sequagel, National Diagnostics) and exposed to X-ray film.

Northern Blot and RT-PCR

Multiple tissue Northern blot was purchased from Clonetech and processed according to the manufacturer's instructions. Total RNA was isolated from selected tissues by acid phenol extraction (RNAzol). PolyA+ was selected by OligodT chromatography, according to standard procedures. PolyA+ RNA (2 μg) was electrophoresed through a formaldehyde-agarose gel and transferred to Nytran membrane. Probes were labeled as above and hybridized for 1 hr in RapidHyb (Clonetech). Blots were washed in 2 × SSC, 0.05% SDS at 18°C and in 0.1 × SSC, 0.1% SDS at 50°C. Reverse transcription reactions were performed in a solution of 0.02 OD random primer, 5 μg RNA, 1× first strand cDNA buffer (GIBCO), 10 mM dithiothreitol, 0.4 mM dNTPs, 40 U RNAsin (Ambion), and 200 U Superscript II (GIBCO) in a volume of 25 μl, at 42°C for 45 min. Of the RT reaction, 2.5–5.0 μl was used in PCR assays using Boehringer HighFidelity PCR kits according to the manufacturer's instructions.

In Situ Analysis

Animals were anesthetized with ketamine (100 μg/gram) and xylazine (10 μg/g) and perfused transcardially with 4% paraformaldehyde in phosphate-buffered saline. Dissected tissue was postfixed at 4°C for 24–72 hr. Paraffin-embedded tissue was cut at 5 μm in sagittal and horizontal planes. Probe preparation, tissue processing, and hybridization were carried out as described (Tessarollo and Parada, 1995). Slides were dipped in Kodak NBT emulsion and exposed for 9 days.

Immunocytochemistry

Tissue fixation was performed as above. Thick vibratome sections cut at 75 μm were processed as described (Ross et al., 1990). Primary antibodies were used at dilutions of 1:2000 (anti-Calbindin), 1:1 (anti-Zebrin), 1:500 (anti-TH). Secondary antibodies were goat anti-rabbit or goat anti-mouse conjugated to peroxidase and were used according to the manufacturer's instructions (Boehringer Mannheim). ApopTag (Oncor, Inc.) staining was performed, according to the manufacturer's instructions, on slide-mounted sections cut at 5 μm from paraffin-embedded tissue. Sections were counterstained with toluidine blue.

Acknowledgments

We thank C. A. Mason and R. Blazeski for invaluable assistance with immunocytochemistry; L. Cleveland, J. D. Dietz, F. L. Dorsey, C. Dunbar, and A. Valenzuela for expert technical assistance; Belinda Harris for providing mutant mice; L. Tessarollo for helpful advice on in situ analysis; S. Ackerman for her cDNA library; F. Qian, U. Kruse, and A. E. Sippel for *Nfix* probe; and D. Koeller for *Gcdh* probe. We thank Dr. J. L. Noebels for many valuable discussions. Research was sponsored by the National Cancer Institute, DHHS, under contract with ABL. The contribution by C. M. L. was in partial fulfillment of a Ph.D. dissertation at the University of Maine and was supported by a DOE-EPSCOR fellowship to C. M. L. and an NIH grant and Klingenstein Fellowship to W. N. F. The contents of this publication do not necessarily reflect the views or policies of the Department of Health and Human Services, nor does the mention of trade names, commercial products, or organizations imply endorsement by the United States Government.

Received September 18, 1996; revised October 21, 1996.

References

Adachi, K., Sobue, I., Tohyama, M., and Shimuzu, N. (1975). Changes in the cerebellar noradrenaline nerve terminals of the neurological murine mutant rolling mouse Nagoya: a histofluorescence analysis. Anat. Hum. Biol. Neurobiol. Neurophysiol. *3*, 329–330.

Anderson, V.E., Rich, S.S., Hauser, W.A., and Wilcox, K.J. (1991). Family studies of epilepsy. In Genetic Strategies in Epilepsy Research, V.E. Anderson, W.A. Hauser, I.E. Leppik, J.L. Noebels, and S.S. Rich, eds. (Amsterdam: Elsevier Science Publishers B.V.), pp. 89–103.

Annegers, J.F. (1991). The use of analytical epidemiological methods in family studies of epilepsy. In Genetic Strategies in Epilepsy Research, V.E. Anderson, W.A. Hauser, I.E. Leppik, J.L. Noebels, and S.S. Rich, eds. (Amsterdam: Elsevier Science Publishers B.V.), pp. 139–164.

Austin, M.C., Schultzberg, M., Abbott, L.C., Montpied, P., Evers, J. R., Paul, S.M., and Crawley, J.N. (1992). Expression of tyrosine

hydroxylase in cerebellar Purkinje neurons of the mutant tottering and leaner mouse. Brain Res. Mol. Brain Res. *15*, 227–240.

Catterall, W.A. (1995). Structure and function of voltage-gated ion channels. Annu. Rev. Biochem. *64*, 493–531.

Chaudhari, N. (1992). A single nucleotide deletion in the skeletal muscle-specific calcium channel transcript of muscular dysgenesis (mdg) mice. J. Biol. Chem. *267*, 25636–25639.

Choi, D.W. (1995). Calcium: still center-stage in hypoxic-ischemic neuronal death. Trends Neurosci. *18*, 58–60.

Christakos, S., Roten, W.B., and Feldman, S.C. (1987). Rat calbindin-D_{28k} purification, quantitation immunocytochemical localization and comparative aspects. Methods Enzymol. *139*, 534–551.

de Curtis, M., and Avanzini, G. (1994). Thalamic regulation of epileptic spike and wave discharges. Funct. Neurol. *9*, 307–326.

Dunlap, K., Luebke, J.I., and Turner, T.J. (1995). Excytotic Ca2+ channels in mammalian central neurons. Trends Neurosci. *18*, 89–98.

Galli, C., Meucci, O., Scorziello, A., Werge, T.M., Calissano, P., and Schettini, G. (1995). Apoptosis in cerebellar granule cells is blocked by high KCl, forskolin, and IGF-1 through distinct mechanisms of action: the involvement of intracellular calcium and RNA synthesis. J. Neurosci. *15*, 1172–1179.

Gavrieli, Y., Sherman, Y., and Ben-Sasson, S.A. (1992). Identification of programmed cell death in situ via specific labeling of nuclear DNA fragmentation. J. Cell. Biol. *119*, 493–501.

Ghosh, A., Ginty, D.D., Bading, H., and Greenberg, M.E. (1994). Calcium regulation of gene expression in neuronal cells. J. Neurobiol. *25*, 294–303.

Gizang-Ginsberg, E., and Ziff, E.B. (1990). Nerve growth factor regulates tyrosine hydroxylase gene transcription through a nucleoprotein complex that contains c-Fos. Genes Dev. *4*, 477–491.

Green, M.C. (1989). Catalog of mutant genes and polymorphic loci. In Genetic Variants and Strains of the Laboratory Mouse, M.F. Lyon and A.G. Searle, eds. (Oxford: Oxford University Press), pp. 12–403.

Green, M.C., and Sidman, R.L. (1962). Tottering-a neuromuscular mutation in the mouse. J. Hered. *53*, 79–94.

Hauser, J.F., and Annegers, J.F. (1991). Genetic strategies in epilepsy research. In Genetic Strategies in Epilepsy Research, V.E. Anderson, W.A. Hauser, I.E. Leppik, J.L. Noebels, and S.S. Rich, eds. (Amsterdam: Genetic Strategies in Epilepsy Research), pp. 45–52.

Hawkes, R., and Gravel, C. (1991). The modular cerebellum. Prog. Neurobiol. *36*, 309–327.

Heckroth, J.A., and Abbott, L.C. (1994). Purkinje cell loss from alternating sagittal zones in the cerebellum of leaner mutant mice. Brain Res. *658*, 93–104.

Hellar, A.H., Dichter, M.A., and Sidman, R.L. (1983). Anticonvulsant sensitivity of absence seizures in the tottering mutant mouse. Epilepsia *24*, 25–34.

Herrup, K., and Wilczynski, S.L. (1982). Cerebellar cell degeneration in the leaner mutant mouse. Neuroscience *7*, 2185–2196.

Hess, E.J., and Wilson, M.C. (1991). Tottering and leaner mutations perturb transient developmental expression of tyrosine hydroxylase in embryologically distinct Purkinje cells. Neuron *6*, 123–132.

Hille, B. (1992). Calcium channels. In Ionic Channels of Excitable Membranes (Sunderland, Massachusetts: Sinauer Associates, Inc.), pp. 83–114.

Jenkins, N.A., Copeland, N.G., Taylor, B.A., and Lee, B.K. (1982). Organization, distribution, and stability of endogenous ecotropic murine leukemia virus DNA in chromosomes of Mus musculus. J. Virol. *43*, 26–36.

Kater, S.B., and Mills, R.L. (1991). Regulation of growth cone behavior by calcium. J. Neurosci. *11*, 891–899.

Kilbourne, E.J., Nankova, E.J., Lewis, E.J., McMahon, A., Osaka, H., Sabban, D.B., and Sabban, E.L. (1992). Regulated expression of the tyrosine hydroxylase gene by membrane depolarization. J. Biol. Chem. *267*, 7563–7569.

Koeller, D.M., DiGiulio, K.A., Angeloni, S.V., Dowler, L.L., Frerman, F.E., White, R.A., and Goodman, S.I. (1995). Cloning, structure, and chromosome localization of the mouse glutaryl-CoA dehydrogenase gene. Genomics *28*, 508–512.

Koh, J.Y., and Cotman, C.W. (1992). Programmed cell death: its possible contribution to neurotoxicity mediated by calcium channel antagonists. Brain Res. *587*, 233–240.

Krawczak, M., Reiss, J., and Cooper, D.N. (1992). The mutational spectrum of single base-pair substitutions in mRNA splice junctions of human genes: causes and consequences. Hum. Genet. *90*, 41–54.

Lennon, V.A., Kryzer, T.J., Griesmann, G.E., O'Suilleabhain, P.E., Windebank, A.J., Woppmann, A., Miljanich, G.P., and Lambert, E.H. (1995). Calcium-channel antibodies in the Lambert-Eaton syndrome and other paraneoplastic syndromes. N. Engl. J. Med. *332*, 1467–1474.

Levitt, P., and Noebels, J.L. (1981). Mutant mouse tottering: selective increase of locus ceruleus axons in a defined single-locus mutation. Proc. Natl. Acad. Sci. USA *78*, 4630–4634.

Limbrick, D.D., Jr., Churn, S.B., Sombati, S., and DeLorenzo, R.J. (1995). Inability to restore resting intracellular calcium levels as an early indicator of delayed neuronal cell death. Brain Res. *690*, 145–156.

Llinas, R., Sugimori, M., Lin, J.W., and Cherksey, B. (1989a). Blocking and isolation of a calcium channel from neurons in mammals and cephalopods utilizing a toxin fraction (FTX) from funnel-web spider poison. Proc. Natl. Acad. Sci. USA *86*, 1689–1693.

Llinas, R.R., Sugimori, M., and Cherksey, B. (1989b). Voltage-dependent calcium conductances in mammalian neurons. The P channel. Ann. N.Y. Acad. Sci. *560*, 103–111.

Marescaux, C., Vergnes, M., and Depaulis, A. (1992). Genetic absence epilepsy in rats from Strasbourg. A review. J. Neural Transm. *35*, 37–69.

Meier, H., and MacPike, A.D. (1971). Three syndromes produced by two mutant genes in the mouse. Clinical, pathological, and ultrastructural bases of tottering, leaner, and heterozygous mice. J. Hered. *62*, 297–302.

Mellentin, J.D., Smith, S.D., and Cleary, M.L. (1989). lyl-1, a novel gene altered by chromosomal translocation in T cell leukemia, codes for a protein with a helix-loop-helix DNA binding motif. Cell *58*, 77–83.

Mori, Y., Friedrich, T., Kim, M.S., Mikami, A., Nakai, J., Ruth, P., Bosse, E., Hofmann, F., Flockerzi, V., Furuichi, T., et al. (1991). Primary structure and functional expression from complementary DNA of a brain calcium channel. Nature *350*, 398–402.

Nishimura, Y. (1975). The cerebellum of rolling mouse Nagoya. Adv. Neurological Sci. *19*, 670–672.

Noebels, J.L. (1984a). Isolating single genes of the inherited epilepsies. Ann. Neurol. *16*, S18–21.

Noebels, J.L. (1984b). A single gene error of noradrenergic axon growth synchronizes central neurones. Nature *310*, 409–411.

Noebels, J.L., and Sidman, R.L. (1979). Inherited epilepsy: spike-wave and focal motor seizures in the mutant mouse tottering. Science *204*, 1334–1336.

Orrenius, S., and Nicotera, P. (1994). The calcium ion and cell death. J. Neural Transm. *43*, 1–11.

Perez-Reyes, E., and Schneider, T. (1995). Molecular biology of calcium channels. Kidney Int *48*, 1111–1124.

Ptacek, L.J., Tawil, R., Griggs, R.C., Engel, A.G., Layzer, R.B., Kwiecinski, H., McManis, P.G., Santiago, L., Moore, M., Fouad, G., et al. (1994). Dihydropyridine receptor mutations cause hypokalemic periodic paralysis. Cell *77*, 863–868.

Qian, F., Kruse, U., Lichter, P., and Sippel, A.E. (1995). Chromosomal localization of the four genes (NFIA, B, C, and X) for the human transcription factor nuclear factor I by FISH. Genomics *28*, 66–73.

Qiao, X., and Noebels, J.L. (1991). Genetic and phenotypic heterogeneity of inherited spike-wave epilepsy: two mutant gene loci with independent cerebral excitability defects. Brain Res. *555*, 43–50.

Rettig, J., Sheng, Z., Kim, D.K., Hodson, C.D., Snutch, T.P., and

Catterall, W.A. (1996). Isoform-specific interaction of the α1A subunits of the brain calcium channels with the presynaptic proteins syntaxin and SNAP-25. Proc. Natl. Acad. Sci. USA *93*, 7363–7368.

Ross, M.E., Fletcher, C., Mason, C.A., Hatten, M.E., and Heintz, N. (1990). Meander tail reveals a discrete developmental unit in the mouse cerebellum. Proc. Natl. Acad. Sci. USA *87*, 4189–4192.

Ryan, S.G. (1995). Partial epilepsy: chinks in the armour. Nat. Genet. *10*, 4–6.

Ryder, K., Lau, L.F., and Nathans, D. (1988). A gene activated by growth factors is related to the oncogene v-jun. Proc. Natl. Acad. Sci. USA *85*, 1487–1491.

Sather, W.A., Tanabe, T., Zhang, J.F., Mori, Y., Adams, M.E., and Tsien, R.W. (1993). Distinctive biophysical and pharmacological properties of class A (BI) calcium channel alpha 1 subunits. Neuron *11*, 291–303.

Snead, O.C. (1995). Basic mechanisms of generalized absence seizures. Ann. Neurol. *37*, 146–157.

Spitzer, N.C., Xianan, X., and Olson, E. (1994). Action potential, calcium transients and the control of differentiation of excitable cells. Curr. Opin. Neurobiol. *4*, 70–77.

Starr, T.V., Prystay, W., and Snutch, T.P. (1991). Primary structure of a calcium channel that is highly expressed in the rat cerebellum. Proc. Natl. Acad. Sci. USA *88*, 5621–5625.

Stea, A., Tomlinson, W.J., Soong, T.W., Bourinet, E., Dubel, S.J., Vincent, S.R., and Snutch, T.P. (1994). Localization and functional properties of a rat brain alpha 1A calcium channel reflect similarities to neuronal Q- and P-type channels. Proc. Natl. Acad. Sci. USA *91*, 10576–10580.

Takahashi, T., and Momiyama, A. (1993). Different types of calcium channels mediate central synaptic transmission. Nature *366*, 156–158.

Tang, S., Mikala, G., Bahinski, A., Yatani, A., Varadi, G., and Schwartz, A. (1993). Molecular localization of ion selectivity sites within the pore of a human L-type cardiac calcium channel. J. Biol. Chem. *268*, 13026–13029.

Tessarollo, L., and Parada, L.F. (1995). In situ hybridization. Methods Enzymol. *254*, 419–430.

Tsakiridou, E., Bertollini, L., de Curtis, M., Avanzini, G., and Pape, H.-C. (1995). Selective increase in T-type calcium conductance of reticular thalamic neurons in the rat model of absence epilepsy. J. Neurosci. *15*, 3110–3117.

Tsien, R.W., Ellinor, P.T., and Horne, W.A. (1991). Molecular diversity of voltage-dependent Ca2+ channels. Trends Pharmacol. Sci. *12*, 349–354.

Urade, Y., Oberdick, J., Molinar-Rode, R., and Morgan, J.I. (1991). Precerebellin is a cerebellum-specific protein with similarity to the globular domain of complement C1q B chain. Proc. Natl. Acad. Sci. USA *88*, 1069–1073.

Usowicz, M.M., Sugimori, M., Cherksey, B., and Llinas, R. (1992). P-type calcium channels in the somata and dendrites of adult cerebellar Purkinje cells. Neuron *9*, 1185–1199.

Volsen, S.G., Day, N.C., McCormack, A.L., Smith, W., Craig, P.J., Beattie, R., Ince, P.G., Shaw, P.J., Ellis, S.B., Gillespie, A., et al. (1995). The expression of neuronal voltage-dependent calcium channels in human cerebellum. Mol. Brain Res. *34*, 271–282.

Wheeler, D.B., Randall, A., Sather, W.A., and Tsien, R.W. (1995). Neuronal calcium channels encoded by the alpha1a subunit and their contribution to excitatory synaptic transmission in the CNS. Prog. Brain Res. *105*, 65–77.

Yang, J., Ellinor, P.T., Sather, W.A., Zhang, J.F., and Tsien, R.W. (1993). Molecular determinants of Ca2+ selectivity and ion permeation in L-type Ca2+ channels. Nature *366*, 158–161.

Zhang, J.F., Randall, A.D., Ellinor, P.T., Horne, W.A., Sather, W.A., Tanabe, T., Schwarz, T.L., and Tsien, R.W. (1993). Distinctive pharmacology and kinetics of cloned neuronal Ca2+ channels and their possible counterparts in mammalian CNS neurons. Neuropharmacology *32*, 1075–1088.

Zheng, J.Q., Felder, M., Connor, J.A., and Poo, M.-M. (1994). Turning of nerve growth cones induced by neurotransmitters. Nature *368*, 140–143.

GenBank Accession Number

The accession number for the sequence reported in this paper is U76716.